UNIVERSITEIT • STELLENBOSCH • UNIVERSITY

On the optimisation of gluconeogenesis by thermophilic species

Davis Marshall Todt [a*]

[a] *Department of Biochemistry, Stellenbosch University, Private Bag X1, Matieland 7602, South Africa*

ARTICLE INFO

Background: A challenge facing thermophilic organisms is the degradation of carbon intermediates of metabolism at high temperatures.
Results: An optimum enzyme activity parameter set was found for the reduced gluconeogenic system in which two-fold improvement of product yield was observed.
Conclusion: The predicted set of parameters indicated that a "pull" rather than "push" approach to system flux was most effective in mitigating carbon loss via thermolabile metabolites.
Significance: Many industrial bioprocesses are carried out at high temperatures and may experience reduced efficiency due to carbon loss via thermolabile intermediates.

ABSTRACT

Thermophilic organisms such as *Sulfolobus solfataricus* grow optimally at temperatures between 60° - 80° C. In order for life to be possible in such extreme environments, adaptations to otherwise thermolabile macromolecules such as DNA, RNA and proteins have accumulated over time within these organisms. Although the influence of the thermostability of macromolecules on metabolism has been studied extensively, few studies have focused on the impact of the degradation of small molecules such as carbon intermediates on metabolism at high temperatures. Recently, it was found that up to 50% of carbon was lost via metabolite instability at 70° C in a reconstituted system of gluconeogenesis by *S. solfataricus*. The reduced system, which monitored carbon flux from 3-phosphoglycerate (3-PG) through to fructose 6-phosphate (F6P), was used to construct a kinetic model which could predict carbon loss within the system via the thermolabile intermediates 1,3-bisphosphoglycerate (BPG), glyceraldehyde 3-phosphate (GAP) and dihydroxyacetone phosphate (DHAP). Product formation was optimized for this system in silico by altering the relative enzyme activities of the model such that carbon loss due to metabolite degradation was minimized. The theoretical predictions were then tested experimentally by reconstituting the four enzymes phosphoglycerate kinase (PGK), glyceraldehyde 3-phosphate dehydrogenase (GAPDH), triose-phosphate isomerase (TPI) and fructose 1,6-bisphosphate aldolase/phosphatase (FBPA/ase) together in an in vitro system at 70° C. These four enzymes, together with the necessary cofactors ATP and NADPH as well as cofactor regenerating enzymes, formed a minimized system in which carbon loss via BPG, GAP and DHAP degradation was monitored using NMR spectrophotometry.

Keywords: pathway efficiency; Sulfolobus solfataricus; systems biology; thermolabile metabolite
Abbreviations: 3-PG, 3-phosphoglycerate; BPG, 1,3-bisphosphoglycerate; DHAP, dihydroxyacetone phosphate; F6P, fructose 6-phosphate; FBPA/ase, fructose 1,6-bisphosphate aldolase/phosphatase; GAP, glyceraldehyde 3-phosphate; GAPDH, glyceraldehyde 3-phosphate dehydrogenase; GDH, glucose dehydrogenase; LMA, Levenberg-Marquardt analysis; MCA, Monte Carlo analysis; NMR, Nuclear Magnetic Resonance, PEP, phosphoenolpyruvate; PGK, phosphoglycerate kinase; PK, pyruvate kinase; TPI, triose-phosphate isomerase.

* Corresponding author.
E-mail address: davistodt@hotmail.com (D.M. Todt).

1. Introduction

Thermophiles have long since captivated scientists from many different spheres of research due to their ability to live at temperatures exceeding 55° C; a feat once considered impossible. While thermophiles are defined as microorganisms which are able to thrive at temperatures exceeding 55°, perhaps even more interesting are the extreme- and hyperthermophiles which grow optimally at temperatures exceeding 75° C and 90° C respectively (Imanaka and Atomi, 2002). Thermophiles are represented primarily by members of the domain archaea, but are also found in deep branching bacteria (Canganella and Wiegel, 2014).

Because of the inherent thermostability of the enzymes they possess, these organisms hold especially high appeal for industrial and pharmaceutical applications which are often carried out at high temperatures (van den Burg, 2003). For this reason, the structural properties of these enzymes which prevent denaturation at high temperatures have been researched extensively in order to elucidate some of their underlying mechanisms. Results of such evaluations have been tentative at best, as very few of these thermodynamic and kinetic properties appear to be conserved between thermostable enzymes (Van den Burg and Eijsink, 2002). It has been suggested, however, that properties such as decreased thermolabile amino acids on the protein surface, increased hydrophobicity in the active site, as well as increased surface charge may all play a role in preventing degradation at high temperatures (Paiardini et al., 2003).

Although the effect of enzyme thermostability on pathway efficiency has been researched extensively, the same cannot be said for carbon intermediates of these pathways. Interestingly, little research has been done on the degradation of these intermediates at such extreme temperatures, which is also intrinsically linked to pathway efficiency. It has been shown previously that many carbon intermediates involved in metabolism are highly unstable at high temperatures. The degradation of these compounds may lead to "carbon loss" from the system via the accumulation of non-metabolisable carbon intermediates (Kouril et al., 2012). Ultimately, this can lead to changes in product yield and system flux.

Sulfolobus solfataricus is an aerobic thermo-acidophile which thrives at temperatures of 80° C at a pH of between 2 to 4 (Zillig et al., 1980). Although much of the central carbon metabolic pathway is conserved in *S. solfataricus*, this organism has developed a host of metabolic adaptations to cope with life at such high temperatures. For glycolysis, the archaeal type branched Entner–Doudoroff (ED) pathway is used. The pathway lacks a functional phosphofructokinase (PFK) enzyme, which is bypassed by substrate channelling via the key intermediate KDG/KDGal through one of two pathways forming pyruvate as end product. Additional enzymes such as the non-phosphorylating glyceraldehyde-3 phosphate dehydrogenase (GAPN) which bypasses production of the extremely thermolabile 1,3-'bisphosphoglycerate (BPG) also represent important adaptations. For gluconeogenesis, the modified Embden–Meyerhof–Parnas (EMP) pathway is used. Possible adaptations of this pathway to high temperatures include the bifunctional fructose 1,6-bisphosphate aldolase/phosphatase (FBPA/ase) enzyme, which is not found in the classical EMP pathway. FBPA/ase catalyses the rapid conversion of the highly thermolabile metabolites glyceraldehyde 3-phosphate (GAP) and dihydroxyacetone phosphate (DHAP) to fructose 6-phosphate (F6P) (Bräsen et al., 2014).

Recently, Kouril et al. showed that the degradation of GAP, DHAP and BPG at 70° C in a reconstituted system of gluconeogenesis for *S. solfataricus* resulted in up to 50% carbon loss from the system (Kouril et al., 2013). The minimal gluconeogenic system (represented in Figure 1) was kinetically modelled and served as a good predictor of metabolite concentrations as well as fluxes through the system. The model can be accessed online at http://jjj.bio.vu.nl/models/kouril3/. By using a systems biology approach, they were able to demonstrate the importance of metabolite stability on the overall efficiency of systems subjected to extreme temperatures.

The efficiency of systems such as these may be optimised for either increased flux or product formation, depending on the intended industrial application. To further apply this knowledge, a project was undertaken with the aim of minimising carbon loss from this system in order to optimise product formation. In this project, the accumulation of F6P was optimised by altering the relative enzyme activities of the system. Since one cannot physically alter the specific activities of the enzymes themselves, the relative enzyme concentrations were altered to increase or decrease activity accordingly. This was achieved by applying various optimisation strategies to simulations using the kinetic model provided by Kouril et al. This paper outlines the two strategies that were applied to optimisation – the Monte Carlo algorithm (MCA) and the Levenberg-Marquardt algorithm (LMA). The MCA or "brute force" approach to optimisation deals with the iterative assignment of random parameters to a model in order to find a global maximum. The LMA makes use of non-linear least squares

regression and is best suited to finding a local maximum, given a close initial starting point. A combination of these strategies was used to predict a theoretical optimum parameter set which would result in maximum F6P production.

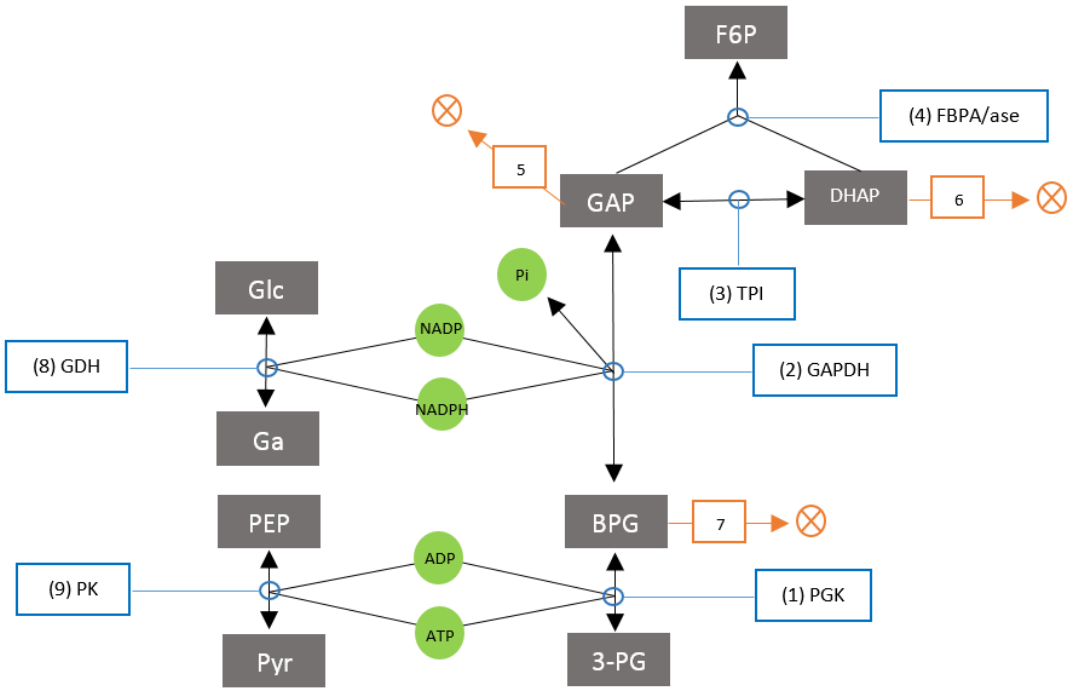

Figure 1: A representation of the metabolic network for the reduced gluconeogenic system modelled by Kouril et al. Reactions 1 – 4 represent the central enzyme catalysed reactions of the pathway in sequence. Reactions 8 and 9 represent the auxiliary reactions required for cofactor regeneration. Reactions 5 – 7 represent the temperature dependent degradation of the three thermolabile metabolites GAP, DHAP and BPG respectively. Green circles, conserved moieties; grey squares, carbon metabolites; open circles, enzyme catalysed reactions; orange crossed-circles, metabolite degradation. FBPA/ase, fructose 1,6-bisphosphate aldolase/ phosphatase; GAPDH, glyceraldehyde 3- phosphate dehydrogenase; GDH, glucose dehydrogenase; PGK, phosphoglycerate kinase; PK, pyruvate kinase; TPI, triosephosphate isomerase.

The optimal parameters predicted using these strategies were then tested by the reconstitution of this reduced pathway in vitro. The production of F6P was assayed using NMR spectrophotometry, which is a novel approach to determining the metabolite concentrations for this system. The results of the *in silico* optimisation approaches as well as the *in vitro* testing of these results will be further discussed in this paper.

2. Materials and Methods

2.1 Model Optimisation

The optimisation algorithm was based on the kinetic model '*kouril3*', which is freely accessible using the JWS online biological systems simulation database (available at: http://jjj.bio.vu.nl/models/kouril3/). Two different optimisation strategies were applied to the model in order to elucidate the optimum parameter set which would result in maximum F6P turnover. Both strategies were aimed at altering the relative enzyme concentrations in the model, while conserving the total enzyme concentration. All other remaining system parameters were left at their default values. All simulations were performed using the *PySCeS (v 0.9.1)* model simulator package (Olivier et al., 2005) in *Python (v 2.7.10)* and the results were rendered using *IPython (v 3.2.1)*. The python package *NumPy (v 1.10.1)* was also used alongside the PySCeS model simulator. Results of both approaches were plotted using either the *matplotlib (1.5.0)* python package, or the *Plotly 2015* web application (Plotly Technologies Inc., 2015).

2.1.1 Optimisation via the Monte Carlo method

For the estimation of a "semi-optimised" state of the model system, an MCA was scripted in the python programming language. The algorithm defines a set of four random enzyme concentrations to be used in the model. The values were drawn from a uniform distribution, in order to ensure that all values had an equal

probability of being selected. The individual values were not limited in range, but were collectively bound by the total enzyme concentration constraint of 49.95 µg/mL, as calculated from the model. The algorithm assigned each of these values to the four corresponding enzyme parameters after which a *PySCeS* simulation was performed for a duration of 200 minutes. Of the 200 time points collected, the maximum F6P concentration was selected and stored for sorting. A total of 2000 iterations were performed.

2.1.2 Optimisation via the Levenberg–Marquardt algorithm

For the determination of the true optimised state for the model, an LMA was scripted in the python programming language. An objective function was created in which the model was simulated for a duration of 200 seconds and the maximum F6P concentration across this interval was selected and returned for minimization. Minimization of the objective function was performed by the *lmfit (v 0.9.2)* python package using non-linear least squares regression. The initial parameter vector was set to the "semi-optimised" parameter set as predicted by the MCA approach. As the goal was to maximize rather than minimize the F6P concentration, the inverse of the result of the objective function was returned for minimization after each successive iteration.

2.2 Expression and isolation of the recombinant enzymes

Recombinant *E. coli* stocks containing plasmids encoding the thermostable enzymes FBPA/ase (EC 4.1.2.13), TPI (EC 5.3.1.1), GAPDH (EC 1.2.1.12), PGK (EC 2.7.2.3), GDH (EC 1.1.1.47), PK (EC 2.7.1.40) and GAPN from *S. solfataricus* were used for culturing and were obtained previously according to the methods by Kouril, T. Overnight cultures of the *E. coli* strains were prepared in 100 mL Erlenmeyer flasks containing 50 mL LB broth (Merck, South Africa). In the case of FBPA/ase, TPI, GAPDH, GDH and PK, cultures were supplemented with 100 µg/mL ampicillin and 34 µg/mL chloramphenicol. The PGK culture was supplemented with 100 µg/mL ampicillin only, while for GAPN 100 µg/mL kanamycin was added. Cultures were grown overnight at 37° C, 180 rpm. The following day, 8 mL of the overnight cultures was added to 1 L Erlenmeyer flasks containing 400 mL LB medium while maintaining the same concentrations of ampicillin, chloramphenicol and kanamycin as before. Cultures were incubated under the same conditions until an optical density of 0.6 was reached (600 nm). Expression was then induced by the addition of 1 mM isopropyl thio-ß-D-galactopyranoside (IPTG) to each of the four cultures, followed by further incubation for 3 hours. Following induction, the cells were harvested by centrifugation (5000 g, 15 min at 4° C) and resuspended in 100 mM Tris/HCl (pH 7.0 at 25° C) in a ratio of 3 mL buffer to 1 g cell pellet. In the case of PGK, 5 mM $MgCl_2$ was also added to the buffer as it was found to have a stabilizing effect on the enzyme and resulted in a higher protein yield. Cells were then lysed by sonication by pulsing for 15 minutes at 4° C. Cell lysates were then placed in Eppendorf tubes and centrifuged at 14 000 g for 20 minutes at 4° C. Supernatants were collected and treated at 80° C for 20 minutes using a heating block in order to denature endogenous *E. coli* proteins. The crude extracts were then centrifuged at 14 000 g for 20 minutes at 4° C and the supernatants containing the heat stable enzymes were collected. Finally, extracts were supplemented with glycerol to a final concentration of 10% (v/v) and stored at -80° C.

2.3 Determination of specific enzyme activity

In order to determine the relative amounts of enzymes to add to the reconstituted system in relation to the values used in the literature, the specific activity of each of the enzymes was deduced. For each assay, the change in NADPH absorbance at 340 nm was monitored at 70° C with a path length of 1 cm (ε_{NADPH} = 5.71 mM^{-1} cm^{-1}) using a temperature controlled spectrophotometer. Assays were performed for 5 minutes or until equilibrium was reached. For all assays, 100 mM Tris/HCl containing 20 mM $MgCl_2$ (pH 6.5 at 70° C) was used as the reaction buffer, and was pre-heated to 75° C in order for all samples to maintain a consistent temperature of 70° C throughout the course of the assay. Assays were performed at a final volume of 1 mL. For all assays, two control steps were performed – the first was to ensure that a constant NADPH absorbance was attained prior to incubation with the substrate. This step ensured that NADPH was stable and that changes in absorbance upon the addition of substrate could be solely attributed to the expected reaction. The second control step involved testing whether a doubling of enzyme concentration would result in an approximate doubling of reaction rate. This step was performed to ensure that the rate of the reaction was not limited by external factors such as the concentration of substrates, cofactors or auxiliary enzymes in the reaction.

2.3.1 FBPA/ase assay

For the FBPA/ase reaction, a coupled enzyme assay was performed using 20µL glucose 6-phosphate isomerase from *Thermoproteus tenax* (Ttx-PGI) and 20 µL glucose 6-phosphate dehydrogenase from *Thermotoga maritima* (Tma-G6PDH) as thermostable auxiliary enzymes. Both Ttx-PGI and Tma-G6PDH were obtained from Kouril, T. In addition, 10 or 20 µL of FBPA/ase was added to the reaction as the rate limiting step, along with 2 mM $NADP^+$ as cofactor, 2 mM DHAP and 2 mM GAP as substrates. The increase in absorbance of NADPH was monitored over 5 minutes to determine the initial rate and subsequently the specific activity of FBPA/ase. The specific activity was compared to the default value of 0.0095 mmol min^{-1} mL^{-1} as found in the model in order to determine the required volume of enzyme to be used in the reconstituted system (Kouril et al., 2013).

2.3.2 TPI assay

TPI activity was monitored via a coupled assay with GAPN as auxiliary enzyme. A 100 x dilution was made of the TPI enzyme in order to monitor activity effectively. Either 20 or 40 µL of GAPN was added to the assay, along with 10 or 20 µL of TPI (100 x diluted) respectively. $NADP^+$ (2mM) was added as a cofactor, along with 0.1 mM glucose 1-phosphate (G1P) and 2 mM DHAP as substrates. The increase in absorbance of NADPH was monitored over a 5 minute interval in order to determine the reaction rate, and subsequently the specific activity of TPI. The specific activity was compared to the value of 0.204 mmol min^{-1} mL^{-1} as found in the literature (Kouril et al., 2013) in order to determine the required volume of enzyme to be used in the reconstituted system.

2.3.3 GAPDH assay

A coupled reaction was performed using PGK as auxiliary enzyme. PGK (20 µL) was added to the reaction, along with 2 or 4 µL GAPDH as the rate limiting enzyme. NADPH (0.2 mM) was added as a cofactor for GAPDH, along with the substrates ATP (10 mM) and 3-PG (5 mM). The decrease in NADPH absorbance was measured over 5 minutes and the reaction rate was determined. Using the reaction rate, the specific activity of GAPDH was determined and compared to the value in the literature (0.869 mmol min^{-1} mL^{-1}) (Kouril et al., 2013).

2.3.4 PGK assay

The same assay was performed as for the GAPDH assay, except that PGK was added in rate limiting concentrations (10 µL or 20 µL) rather than GAPDH which was added in excess (40 µL). The decrease in NADPH absorbance was measured over 2 minutes and the specific activity of PGK was calculated. The specific activity was then compared to the specific activity for PGK as found in the literature (0.0589 mmol min^{-1} mL^{-1}) (Kouril et al., 2013).

2.4 P-31 NMR assay of the optimised reconstituted system

All enzymes and reagents including the substrate, 3-PG were added to the reaction tube for incubation prior to NMR analysis. The four enzymes FBPA/ase, TPI, GAPDH and PGK were added to the reaction tube in volumes relative to the concentration parameter set predicted by the MCA-LMA optimisation (see Results), taking into account fold changes in activity between experimentally determined values and those found in the literature (Kouril et al., 2013). The two auxiliary enzymes GDH and PK were added at volumes equal to that of GAPDH and PGK (i.e. 25.94 and 83.88 µL, respectively). In addition, 20 mM $MgCl_2$, 10 mM ATP, 0.2 mM NADPH, 10 mM D-glucose and 146.81 µL of Tris/HCl (0.1 M, pH 6.5 at 70° C) were added. A final concentration of 2mM 3-PG was added as substrate. Finally, triethyl phosphate (TEP) was added as a known standard to a final concentration of 5 mM, along with 100 µL of 100% D_2O. Assays were prepared to a final volume of 1 mL.

The assay was incubated at 70° C for 3 hours using a heating block. The sample was subjected to 600 MHz NMR spectrophotometry at 14° C and allowed to proceed for 12 hours. Additionally, an assay containing three times the GAPDH and GDH concentration and one third of the PGK and PK concentrations was incubated under identical conditions. This was then subjected to 400 MHz NMR spectrophotometry at 21° C for 3 hours. A 1.6 second acquisition time followed by a 40 second relaxation time was used for both assays. To reduce noise, 1 Hz apposition was performed on the spectra.

3. Results

3.1 Optimisation via the Monte Carlo method

The complete MCA/LMA script, along with a version in pseudocode can be accessed online at http://tinyurl.com/gluconeogenesisoptimisation. The results of the optimisation are shown in Figure 2, below.

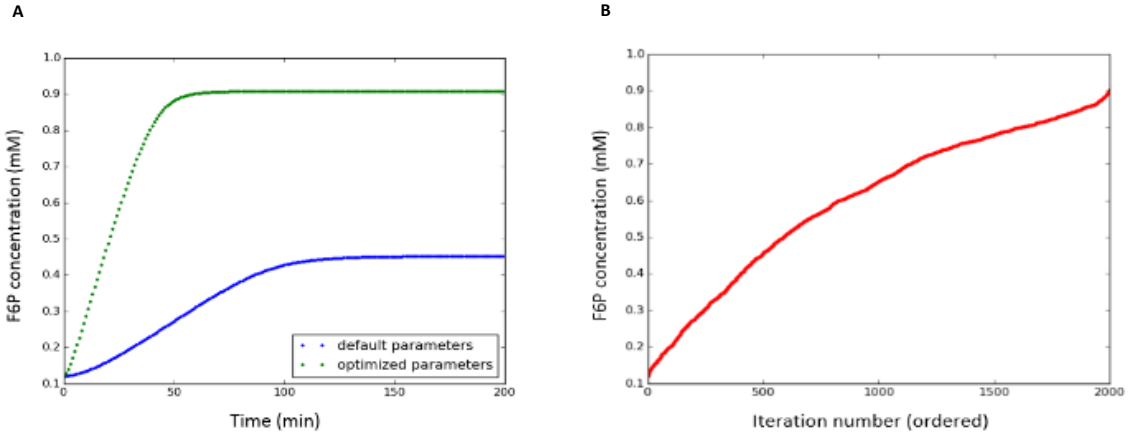

Figure 2: Results of optimisation using the Monte Carlo approach. A, the accumulation of F6P (mM) as a function of time (min) for a single model simulation using either the default parameter values used in the model (blue), or the optimal parameters as predicted by the MCA (green). B, the maximum F6P concentration (mM) accumulated over 200 minutes for each of the 2000 simulations using random parameters adding up to the total enzyme constraint. The values are ordered from lowest to highest F6P concentration.

When the model was simulated using the default values for all parameters, a maximum F6P concentration of 0.4520 mM was obtained from the model (Figure 2a). However, when the model was fitted with parameters predicted by the MCA simulation, a maximal F6P value of 0.9083 mM was observed, indicating an approximate 2 fold increase of F6P production for the optimised system. This value readily approaches the theoretical maximum of 1 mM, as calculated from molar ratios for the reaction when metabolite degradation is not taken into account (2 mM of 3-PG is converted to 1 mM of F6P under ideal conditions). Figure 2b represents the complete data set obtained by the MCA for 2000 iterations using random parameters. The graph indicates a logit, or inverse sigmoidal distribution of F6P values as expected. The distribution of parameter sets resulting in mid-range F6P values is far wider than boundary values, as small perturbations occurring at the boundary result in minimal increase (in the case of high F6P concentrations) or decrease (in the case of low F6P concentrations) due to the probabilistic nature of the system. The same result was obtained when a subsequent series of simulations were performed involving 3000, 5000 and 10 000 iterations (not shown), in which there was little to no improvement to the maximum F6P produced.

Figure 3 displays the results of the MCA simulation for F6P as a function of the individual enzyme concentrations in the semi-optimised system. It is evident from Figure 3a that for the TPI enzyme, low enzyme concentrations are equally effective in producing a high F6P yield as higher concentrations. Even concentrations approaching 0 mM appear to result in a relatively high F6P production. This can be attributed to TPI's rapid rate of catalysis, meaning that relatively little enzyme is required for the reaction to reach equilibrium (Kouril, T., 2013). However, it is apparent that at the high end of the spectrum for TPI concentration, F6P production is severely hampered or altogether absent. This may be due to the fact TPI experiences strong inhibition by high concentrations of PEP and 3-PG (Kouril, T., 2013), which remains the case when less PGK and PK are available for PEP and 3-PG consumption. Similar observations can be made for the GAPDH enzyme concentration (Figure 3b). It too appears to influence the F6P yield minimally, although comparatively less F6P is produced at very low concentrations of GAPDH, due to its lower maximal rate.

Although TPI and GAPDH concentration appear to play only a minor role on F6P yield, the same is not true for the entry and exit enzymes of the pathway (i.e. PGK and FBPA/ase respectively). Figure 3 c, d shows the maximal F6P production for each of the PGK/FBPA/ase enzyme pairs. It is evident that the F6P yield increases proportionally with an increase in FBPA/ase. This is in contrast to PGK, which is required in smaller concentrations and does not appear to exhibit much control on the system. The optimal ratio is therefore one

in which the FBPA/ase is high and the PGK exists in medium to low concentrations. This is illustrative of a system in which a "pull" rather than a "push" approach exhibits more control over system flux.

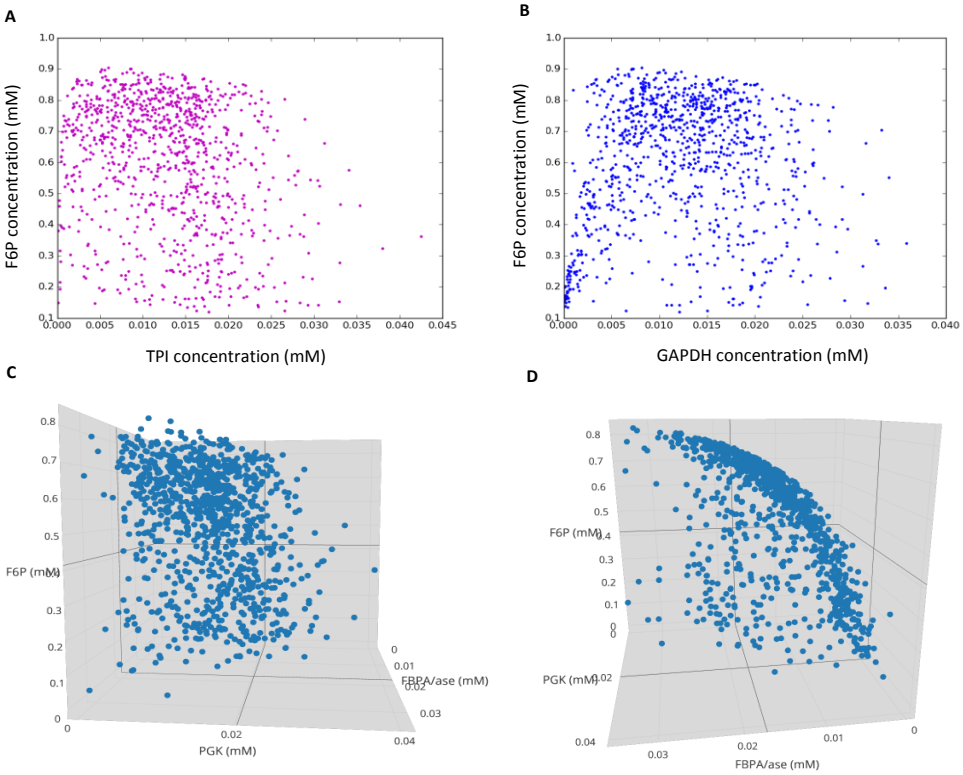

Figure 3: Results of optimisation using the Monte Carlo approach, showing F6P concentration (mM) as a function of individual enzyme concentrations. A and B, the F6P concentrations (mM) corresponding to changes in TPI as well as GAPDH concentration (mM) as extracted from the MCA for 2000 iterations. C and D, a three dimensional scatter plot illustrating the relationship between F6P production (mM) and the PGK/FBPA/ase concentrations for each of 2000 iterations.

3.2 Optimisation via the Levenberg-Marquardt Algorithm

Following the MCA approach to optimisation in which a global maximum was found, an LMA approach was used to find the local maximum. Using the resulting parameter set obtained from MCA as the initial parameter estimation, a local maximum was found at 0.9095 mM F6P. This represents only a minor increase from the 0.9083 mM result obtained from MCA. The final optimisation results are presented in table 1, below. The optimized model is available online at http://jjj.bio.vu.nl/models/kouril3optimized-user/.

Table 1: Parameter values and resulting F6P yield after optimisation with the Levenberg-Marquardt algorithm.

Enzyme	Optimal concentration (mM)	F6P yield (mM)
ALDPA/ase	0.03426	0.9095
GAPDH	0.00473	
PGK	0.00598	
TIM	0.00498	

3.3 NMR assay of the reconstituted gluconeogenic system

The results of the NMR assays of the reconstituted *in vitro* system were largely inconclusive. Table 2 displays the results obtained from NMR spectroscopy using the optimised enzyme parameters as determined for the system. Although the peaks were well enough resolved, no F6P was detected. It is evident that very little of the original 3-PG substrate was consumed in the reaction (1.769 mM remaining from 2 mM). However, the same is not true for PEP, of which only 1.786 mM remained from the original 5 mM. This indicates that at a minimum, reaction 9 of the pathway proceeded as expected. Because the reaction was allowed ample time

to react (3 hours required to reach equilibrium, as predicted by the model), it is possible that too little GAPDH and/or GDH activity was present to catalyse subsequent reactions in the pathway. This would result in the consumption of 3-PG while subsequent BPG formation would simply be degraded due to its extreme thermolability – ultimately leading to no F6P formation. Since it has been postulated that BPG degrades back to 3-PG (Kouril et al., 2012), this may account for the seemingly little 3-PG consumption in the system.

Table 2: Metabolite concentrations in the reconstituted system using the optimised parameters obtained from MCA-LMA analysis as determined by P-31 NMR spectroscopy.

Metabolite	Initial concentration (mM)	Final concentration (mM)
3-PG	2 mM	1.769
ATP	10 mM	8.257
PEP	5 mM	1.786
F6P	0 mM	-

The incubation that followed using increased GAPDH/GDH as well as proportionally lower PGK/PK concentrations resulted in somewhat improved results (Figure 4). F6P was detected, albeit in very low concentrations (0.030 mM). Although this reflects only a minor improvement on the system, it may further indicate that the low activities of GAPDH and GDH were responsible for the failure of the optimisation experiment. However, the fact that less of the substrates 3-PG and ATP were consumed implies that the altered PGK and or PK activities (catalysing steps 1 and 9 in the pathway, respectively) may have been too low in the altered optimisation model. Additionally, having too little PGK activity would have meant that TPI was inhibited strongly by 3-PG throughout the incubation. This would further help to explain the low yield of F6P. The optimum solution is likely one in which the GAPDH/GDH activities are higher than that used in the optimised assay, while the PGK/PK activities are left unchanged.

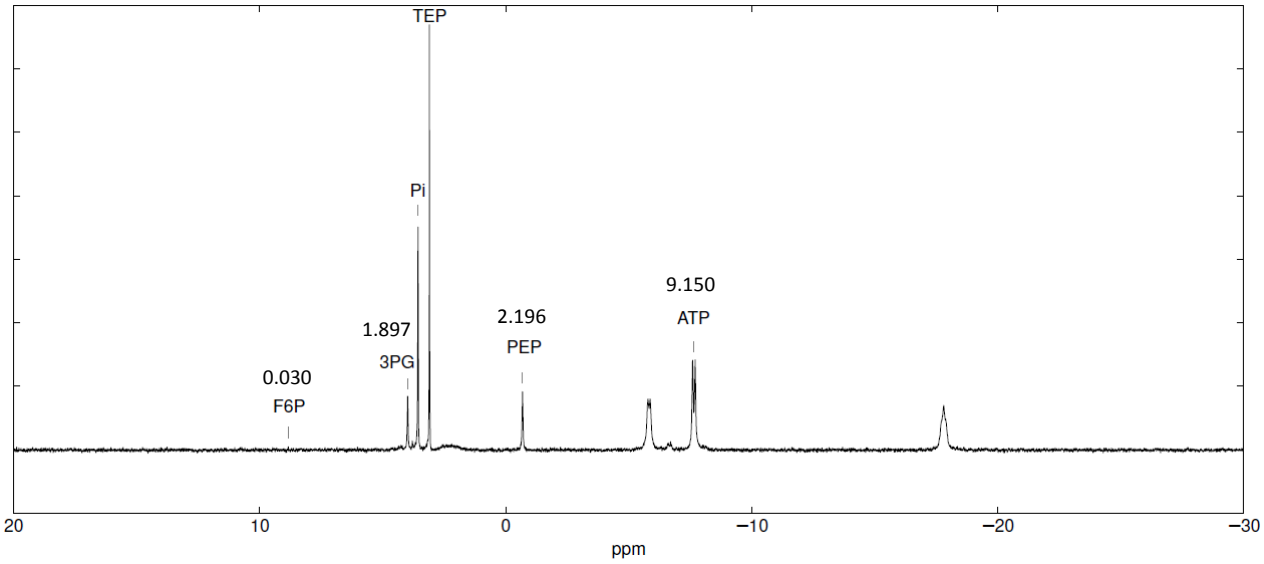

Figure 4: NMR spectrum of the reconstituted system using triple the GAPDH and GDH concentrations as well as a third of the PGK and PK concentrations as the optimal parameter set. Concentrations are in mM. TEP, the internal standard triethyl phosphate of known concentration; Pi, inorganic phosphate.

4. Discussion

Thermostable enzymes have been applied to various spheres of industrial processing, many of which are carried out under extreme temperatures. Their significance as biological agents rather than often expensive or dangerous chemical catalysts means that their use is both widespread and well researched. In industry, these enzymes have been applied to food processing, detergents, leather and textiles, pharmaceuticals, and biofuel production amongst others (Kirk et al., 2002). The carbon intermediates of reactions catalysed by these enzymes have also been shown to be important in the consideration of thermostability within a system. This

has been largely overlooked until recently. Specifically, it has been shown that metabolites such as BPG, GAP and DHAP are extremely vulnerable to degradation at high temperatures, with half times at 70° C of 0.655, 12.4 and 30.8 minutes respectively (Kouril et al., 2013). It has been further demonstrated that the degradation of these metabolites to non-metabolisable "dead-end" compounds can have significant effects on fluxes through the system. These three metabolites are largely conserved between domains due to apparent thermodynamic constraints. As such, the degradation of these metabolites to dead-end compounds may have far reaching consequences for biological as well as industrial systems which operate at extreme temperatures.

This study sought to find an optimised set of parameters for a previously characterised system of gluconeogenesis in which the production of F6P was maximised. The approach taken was to alter the relative enzyme activities of the system (via modifying the enzyme concentrations) in order to redirect the flux of the system to one in which the extent of carbon loss via thermal degradation was minimised. In order to achieve this, two optimisation approaches were applied to the existing model.

The MCA approach was chosen as a useful tool for finding the local maximum of the model. The results of the MCA predicted a suitable parameter set which resulted in an approximate doubling of F6P yield. By deconstructing the resulting data, various trends in the control of the system were also demonstrated. For the intermediate enzymes GAPDH and TPI, it was shown that changes in enzyme concentration had little impact on the accumulation of F6P. This indicates that neither of these enzymes exhibit a great deal of control on the flux of the system. Important to note is the general absence of F6P accumulation at very high TPI concentrations due to inhibition from high PEP and 3-PG concentrations. This represents one of several possible adaptations to life at high temperatures for *S. solfataricus*. When the entry and exit enzymes in the pathway, PGK and FBPA/ase were compared, it was found that PGK activity exhibited little control over pathway flux compared to FBPA/ase. It is evident that FBPA/ase exhibits the greatest control over system flux of the four enzymes – this is illustrative of a "pull" rather than "push" system.

The LMA approach exhibited seemingly insignificant improvements on F6P yield over MCA. The optimal parameter set found appeared to deviate slightly depending on the MCA prediction used as initial estimation for the algorithm. However, it was observed in most cases that the F6P result after parameter tweaking with LMA did represent at least some improvement over the initial MCA values. These differences would be undetectable using NMR analysis. The reason for deviation is likely due to the nature in which the total enzyme constraint was applied to the four enzymes in the objective function. A change in the value of one parameter intrinsically results in compensation for this change by altering the value of another parameter. Since all four parameters are linked in this way, the least squares function is likely to "miss" values along the sum squared residual gradient.

Following optimisation, the resulting parameter set was tested via a reconstituted *in vitro* experiment. The NMR spectroscopy results of the experiment failed to support the predictions performed *in silico*. In all cases, the F6P produced was either undetectable or too low to support the prediction. However, it was discerned from the results that the activity of GAPDH and/or the cofactor regenerator GDH may have simply been too low to allow for the effective conversion of BPG to GAP. It should be noted that the high concentrations of PEP and 3-PG on the inhibition of TPI may have played a supporting role in the low product turnover rate. Since the model was shown to be reliable in the literature, it is unlikely that there exists a fault in parameter prediction via the optimisation approach. In future, the specific activities of enzymes will be more closely compared to the literature values, so as to eliminate calculation or observation errors used in the experimental approach.

Indeed, the same optimisation approach may be further applied to other metabolic pathways of *S. solfataricus*, in order to optimize several useful industrial applications of this organism. Such applications include starch processing and biofuel production via thermostable glucanase and xylanase enzymes in the breakdown of cellulose and hemicellulose (Bräsen et al., 2014). In particular, thermostable glucoamylases derived from *S. solfataricus* have seen huge commercial success in the production of high fructose corn syrup (Kirk et al., 2002). In addition, *S. solfataricus* has also been applied to the production of many pharmaceutical compounds such as the chemotherapeutic carbocyclic nucleosides from γ–lactamase which are used as antiviral agents (Littlechild, 2011).

Since the metabolites used in these central carbohydrate metabolic pathways are largely conserved between domains, they therefore represent an important target for pathway optimization. By taking thermal degradation of these metabolites into account, the application of these enzymes becomes significantly more relevant in industry. This work may therefore have extensive applications in industrial bioprocesses.

5. Conclusion

Thermophilic organisms such as *S. solfataricus* have evolved adapted metabolic pathways in order to survive life at high temperatures. These adaptations include substrate channelling, changes in allostery and the presence of enzymes which are resistant to heat degradation. In addition to macromolecular structures such as DNA, RNA and proteins, low molecular weight molecules are also vulnerable to degradation. Carbon intermediates such as BPG, GAP and DHAP are largely conserved between domains and represent three examples of highly thermolabile intermediates. Using an existing kinetic model of gluconeogenesis for *S. solfataricus*, it was shown here that the optimisation of a system at 70° C in which the enzyme activities were altered appropriately can result in significant improvements to pathway efficiency for the system. It was found using an *in silico* approach that the yield of the product, F6P, could theoretically be doubled in comparison to when model default parameters were used. The increase in yield can be attributed to a decreased rate of metabolite degradation at high temperatures. This serves as a useful example of the importance of metabolite thermo-stability when the optimisation of biological or industrial processes is being considered.

6. References

Bräsen, C., Esser, D., Rauch, B., Siebers, B., 2014. Carbohydrate metabolism in Archaea: current insights into unusual enzymes and pathways and their regulation. Microbiol. Mol. Biol. Rev. 78, 89–175. doi:10.1128/MMBR.00041-13

Canganella, F., Wiegel, J., 2014. Anaerobic Thermophiles. Life 4, 77–104. doi:10.3390/life4010077

Imanaka, T., Atomi, H., 2002. Catalyzing " Hot " Reactions : Enzymes from Hyperthermophilic Archaea 149–163. doi:10.1002/tcr.10023

Kirk, O., Borchert, T.V., Fuglsang, C.C., 2002. Industrial enzyme applications. Curr. Opin. Biotechnol. 13, 345–351. doi:10.1016/S0958-1669(02)00328-2

Kouril, T., Esser, D., Kort, J., Westerhoff, H. V, Siebers, B., Snoep, J.L., 2013a. Intermediate instability at high temperature leads to low pathway efficiency for an in vitro reconstituted system of gluconeogenesis in Sulfolobus solfataricus. FEBS J. 280, 4666–80. doi:10.1111/febs.12438

Kouril, T., Esser, D., Kort, J., Westerhoff, H. V., Siebers, B., Snoep, J.L., 2013b. Intermediate instability at high temperature leads to low pathway efficiency for an in vitro reconstituted system of gluconeogenesis in Sulfolobus solfataricus. FEBS J. 280, 4666–4680. doi:10.1111/febs.12438

Kouril, T., Kolodkin, A., Zaparty, M., Steuer, R., Ruoff, P., Westerhoff, H. V, Snoep, J., Siebers, B., Sulfo, S.Y.S.C., 2012. Sulfolobus Systems Biology: Cool Hot Design for Metabolic Pathways.

Littlechild, J. a, 2011. Thermophilic archaeal enzymes and applications in biocatalysis. Biochem. Soc. Trans. 39, 155–158. doi:10.1042/BST0390155

Olivier, B.G., Rohwer, J.M., Hofmeyr, J.-H.S., 2005. Modelling cellular systems with PySCeS. Bioinformatics 21, 560–1. doi:10.1093/bioinformatics/bti046

Paiardini, A., Gianese, G., Bossa, F., Pascarella, S., 2003. Structural plasticity of thermophilic serine hydroxymethyltransferases. Proteins 50, 122–34. doi:10.1002/prot.10268

van den Burg, B., 2003. Extremophiles as a source for novel enzymes. Curr. Opin. Microbiol. 6, 213–218. doi:10.1016/S1369-5274(03)00060-2

Van den Burg, B., Eijsink, V.G., 2002. Selection of mutations for increased protein stability. Curr. Opin. Biotechnol. 13, 333–337. doi:10.1016/S0958-1669(02)00325-7

Zillig, W., Stetter, K.O., Wunderl, S., Schulz, W., Priess, H., Scholz, I., 1980. The Sulfolobus-"Caldariella" group: Taxonomy on the basis of the structure of DNA-dependent RNA polymerases. Arch. Microbiol. 125, 259–269. doi:10.1007/BF00446886